

## Inelastic excitation of giant resonances by 400-MeV $^{16}\text{O}$

T. P. Sjoreen, F. E. Bertrand, R. L. Auble, E. E. Gross, D. J. Horen, D. Shapira, and D. B. Wright\*

*Oak Ridge National Laboratory, Oak Ridge, Tennessee 37830*

(Received 3 November 1983)

Results are presented for 350- and 400-MeV  $^{16}\text{O}$  inelastic scattering from  $^{208}\text{Pb}$  and  $^{90}\text{Zr}$ . The results show excitation of the giant quadrupole, monopole, and dipole resonances. The cross section and peak to continuum ratio are very large for the giant quadrupole resonance. Measured angular distributions agree with distorted-wave Born approximation calculations which use standard collective model form factors. Structure observed in the  $^{16}\text{O}$  spectra corresponding to high excitation energies in  $^{208}\text{Pb}$  is shown to arise from projectile pickup reactions.

### I. INTRODUCTION

During the last decade several new giant resonances have been observed and systematics for some of them have been established. In particular, much has been learned about the isoscalar giant monopole resonance (GMR) and the giant quadrupole resonance (GQR). The giant resonance work of the last decade is summarized in several recent review papers.<sup>1-3</sup> Much of the successful classification can be attributed to the variety of probes used in giant resonance measurements. These probes include elec-

trons and pions as well as light ions, viz., protons, deuterons,  $^3\text{He}$ , and alpha particles. One probe which has not been used extensively is heavy ions. The potential advantages (and disadvantages) of heavy ions for exciting giant resonances have been pointed out previously.<sup>4,5</sup> However, little data have been taken due largely to the lack of heavy ion beams having sufficient energy to provide resonance cross sections comparable with those achieved with lighter ions. At higher bombarding energies giant resonance cross sections from heavy-ion inelastic scattering are expected to be enhanced considerably. For example, the distorted-wave born approximation (DWBA) calculations shown in Fig. 1 for inelastic scattering of  $^{16}\text{O}$  from  $^{208}\text{Pb}$  indicate that the cross section at the grazing angle for  $L=2$  and 4 multipolarities should increase by an order of magnitude as the bombarding energy is increased from 10 to 25 MeV/nucleon. In addition, the continuum is expected to be relatively smaller with heavy ions because knockout reactions should be greatly reduced in importance.<sup>5</sup> This feature, coupled with larger cross sections, suggests that very favorable peak to backgrounds may be obtained with medium energy heavy ions. As yet, however, little work<sup>6-8</sup> has been done with heavy ions, and most of these studies have been done at beam energies  $\leq 20$  MeV/nucleon.

Recently, heavy ion beams with energies up to 25 MeV/nucleon for  $A < 40$  have become available at the Holifield Heavy Ion Research Facility (HHIRF). As indicated by the DWBA calculations in Fig. 1, these beams should strongly excite isoscalar giant resonances. In this paper we report on the results of the excitation of giant resonances by inelastic scattering of 350 and 400 MeV  $^{16}\text{O}$  beams from HHIRF.

### II. EXPERIMENTAL PROCEDURE

Giant resonances in  $^{90}\text{Zr}$  and  $^{208}\text{Pb}$  were excited in the present measurements by inelastic scattering of 350- and 400-MeV  $^{16}\text{O}$  ions provided by the coupled operation of the tandem and cyclotron at HHIRF. Differential cross sections were measured at several angles between  $8^\circ$  and  $19^\circ$  (lab) for  $^{208}\text{Pb}$  and  $8^\circ$  and  $14^\circ$  for  $^{90}\text{Zr}$ . The  $^{208}\text{Pb}$  targets were enriched (99%) self-supporting foils 0.8 and 2.0 mg/cm<sup>2</sup> thick, and the  $^{90}\text{Zr}$  target, also a self-supporting

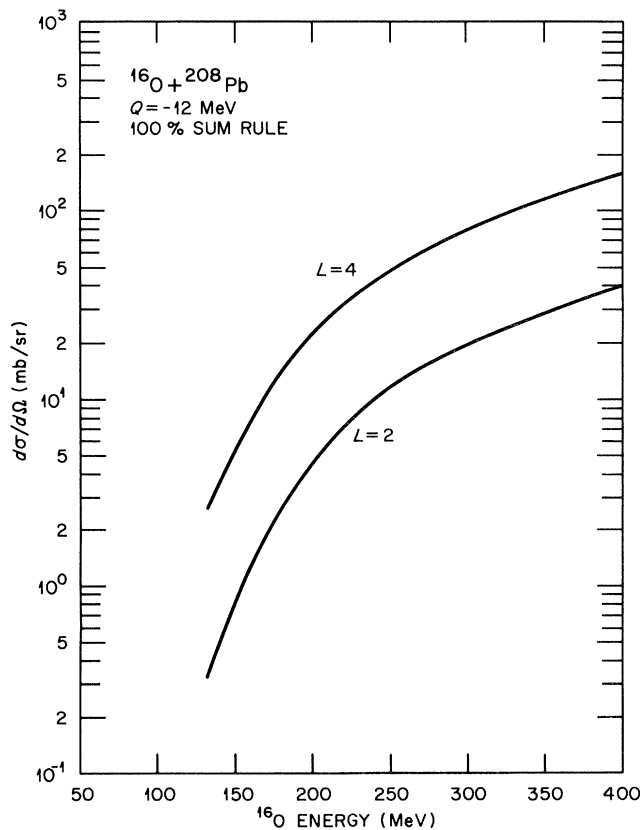


FIG. 1. Calculated  $L=2$  and  $L=4$  cross sections for the ( $^{16}\text{O},^{16}\text{O}'$ ) reaction at a variety of incident energies. The calculations are normalized to 100% of the  $L=2$  and  $L=4$  sum rules.

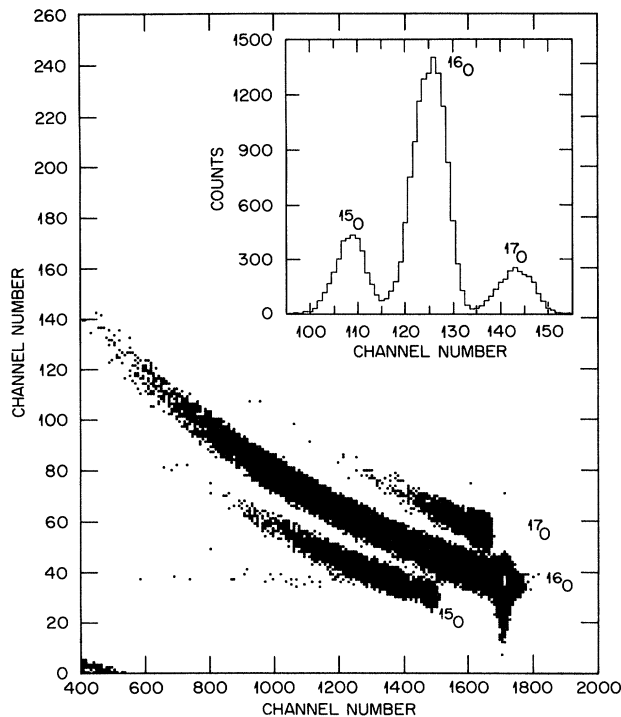


FIG. 2.  $\Delta E \times E$  spectra for oxygen isotopes from the  $^{208}\text{Pb}(^{16}\text{O}, ^{16}\text{O}')$  reaction at 400 MeV. The  $\Delta E$  projection is made for an excitation energy of  $\sim 10$ – $30$  MeV in  $^{208}\text{Pb}$ .

foil, was  $2 \text{ mg/cm}^2$  thick.

The scattered charged particles were detected by cooled, two-element, silicon, surface-barrier detector telescopes consisting of  $500 \mu\text{m}$   $\Delta E$  and  $1500 \mu\text{m}$   $E$  detectors of  $150 \text{ mm}^2$  area. The scattering angle subtended by the telescope collimators was typically  $1.3^\circ$ . The excitation energy range of these telescopes for 400-MeV  $^{16}\text{O}$  ions was about 80 MeV in the inelastic channel. The mass resolution obtained for the oxygen isotopes is illustrated by the  $\Delta E$ - $E$  plot in Fig. 2 and by a projection (insert) of those events which have the same energy loss as the inelastically scattered  $^{16}\text{O}$  ions in the giant resonance region (10–30 MeV excitation). As indicated by the figure, the  $^{16}\text{O}$  particles are well resolved from  $^{15}\text{O}$  and  $^{17}\text{O}$ .

The overall energy resolution was typically about 550 keV FWHM. The four primary contributions to this resolution were the intrinsic response of the detectors, the beam energy spread, the energy-loss straggling in the target, and kinematic broadening. During some runs the energy resolution was 450 keV, for which the estimated beam energy spread was about 150 keV FWHM ( $\Delta E/E = 3.8 \times 10^{-4}$ ). With  $\leq 550$  FWHM energy resolution, it was possible to extract elastic cross sections for  $^{90}\text{Zr}$  and  $^{208}\text{Pb}$  and inelastic cross sections for the 2.61 MeV  $3^-$  state in  $^{208}\text{Pb}$ .

Angle to angle normalization was achieved with fixed angle monitor detectors and the absolute normalization was determined by integration of the charge deposited by the incident beam in a Faraday cup that was biased to  $-300$  V for electron suppression.

The signals from the electronics were digitized and pro-

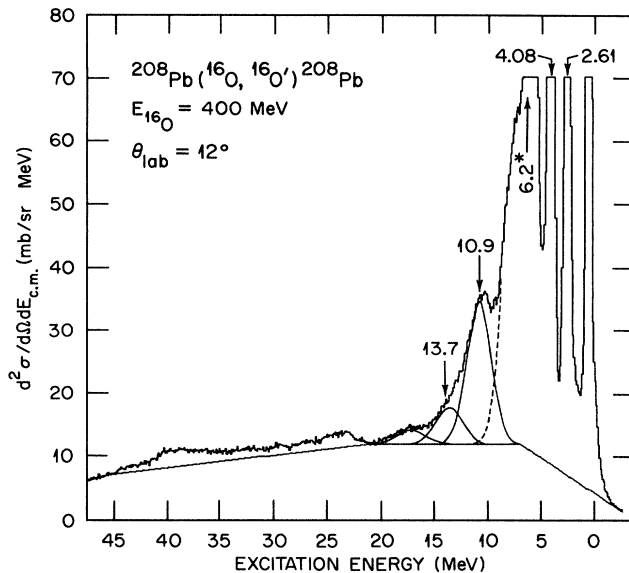


FIG. 3. Inelastic scattering spectrum at 12 deg from the  $^{208}\text{Pb}(^{16}\text{O}, ^{16}\text{O}')$  reaction at 400 MeV. The solid curves show a decomposition of the spectrum into resonance peaks and an underlying continuum.

cessed with the HHIRF data acquisition computer system and ancillary software.<sup>9</sup> The computer deadtime was determined by two methods: (1) A pulser signal was triggered by the monitor counter and processed along with the physical events, and the ratio of pulser triggers to processed pulser events was then taken as a measure of the deadtime; and (2) the total number of events processed by the computer system was scaled along with the total number of event triggers and the ratio of these two numbers was taken as a measure of the deadtime. The two methods gave excellent agreement in the deadtimes, which varied between 5% and 30%. Measurements were made with blank target frames to make sure that no spurious background was present.

### III. EXPERIMENTAL RESULTS

The  $^{16}\text{O}$  spectra obtained from the bombardment of  $^{208}\text{Pb}$  and  $^{90}\text{Zr}$  by 400 MeV  $^{16}\text{O}$  ions show that giant resonances are strongly excited from  $\sim 10$  to 19 MeV in  $^{208}\text{Pb}$  and from 12 to 23 MeV in  $^{90}\text{Zr}$ . The GQR at 10.9 MeV in  $^{208}\text{Pb}$  and at 14.0 MeV in  $^{90}\text{Zr}$  is particularly evident.

Figure 3 is the  $^{16}\text{O}$  inelastic scattering spectrum obtained at  $12^\circ$  (lab) with the  $2.0 \text{ mg/cm}^2$   $^{208}\text{Pb}$  target at 400 MeV bombarding energy. The peak on the far right is from the tail of the elastic peak, most of which has been eliminated by a single channel discriminator. The peak at 2.6 MeV is the  $3^-$  state, and that at 4.1 MeV should be a combination of the 4.08-MeV  $2^+$  state and the 4.32-MeV  $4^+$  state. The broad structure between 5- and 10-MeV excitation is due to excitation of both the target and the  $^{16}\text{O}$  projectile.

Contributions to the spectra from projectile excitation are primarily due to the 6.13 MeV  $3^-$  and 6.92 MeV  $2^+$  states, which are Doppler broadened with widths of  $\sim 3$



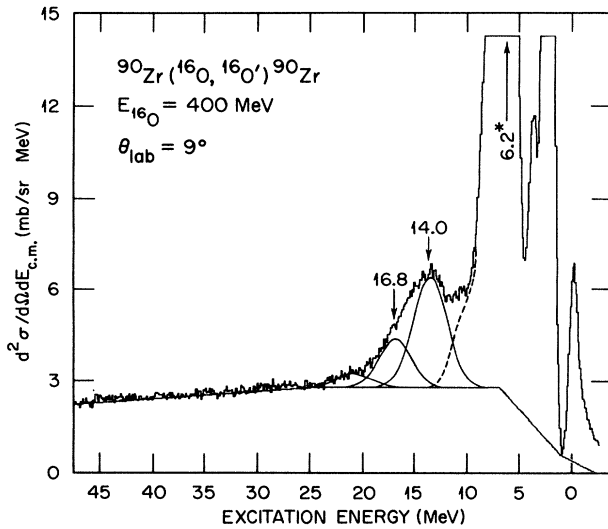


FIG. 5. Inelastic scattering spectrum at 9 deg from the reaction  $^{90}\text{Zr}(^{16}\text{O}, ^{16}\text{O}')^{90}\text{Zr}$  at 400 MeV. The solid curves show a decomposition of the spectrum into resonance peaks and an underlying continuum.

observed which was suggested to be a  $3^-$ ,  $5^-$  giant resonance (GR) excitation. No evidence for such a peak is found in either our 400- or 350-MeV data. We interpret the peak at 19.7 MeV reported in Ref. 7 to be the same as the peak observed at  $\sim 21$  MeV in the present 350 MeV spectra and at  $\sim 23.5$  MeV in the 400 MeV spectra, i.e., it

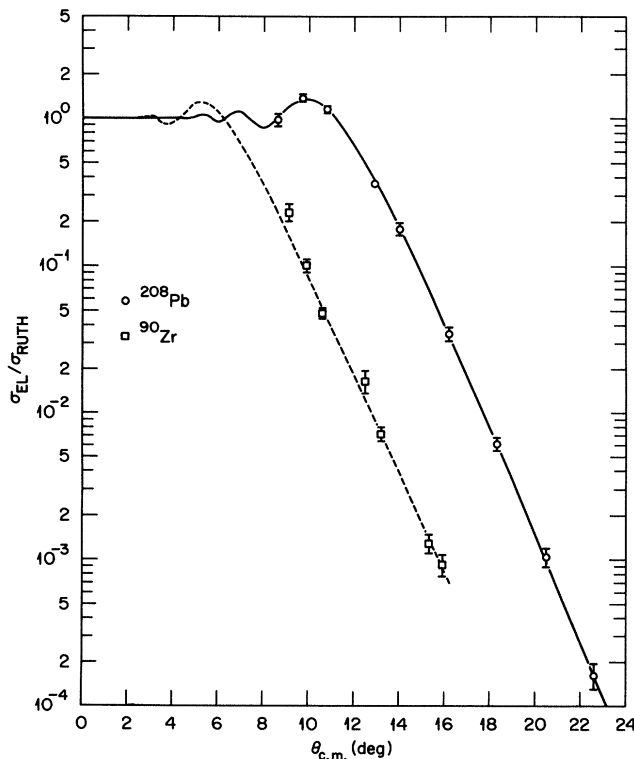


FIG. 6. Elastic scattering angular distributions for the 400 MeV  $^{16}\text{O}$  ions on  $^{208}\text{Pb}$  and  $^{90}\text{Zr}$  compared with fits from the computer code PTOLEMY.

is an artifact of the decay of the pickup channels. In addition, no evidence for a peak at 19.7 MeV excitation in  $^{208}\text{Pb}$  was seen in a  $(^{14}\text{N}, ^{14}\text{N}')$  measurement at 266-MeV bombarding energy.<sup>8</sup>

Figure 5 is the spectrum obtained at 9° (lab) with the 2 mg/cm<sup>2</sup>  $^{90}\text{Zr}$  target at 400 MeV bombarding energy. The giant resonance region from 10 to 23 MeV was analyzed in the same way as that for  $^{208}\text{Pb}$ . The only difference being that (1) the flat continuum background was normalized at 23 MeV excitation, and (2) the fixed widths for the GQR and GMR-GDR sum were set at 3.6 and 3.8 MeV, respectively. The extracted excitation energies of 14.0 MeV for the GQR and 16.0 MeV for the GDR + GMR sum agree well with values from other measurements, 14.0-, 16.8-, and 16.8-MeV for the GQR, GMR, and GDR, respectively. A peak with a centroid at 23-MeV excitation and width of  $\sim 5$  MeV was also extracted. The results of the fitting procedure are denoted by the solid lines in Fig. 5, while the dashed line represents the “tail” of the low lying excited states, projectile excitations, and a residue of counts near 9-MeV excitation. This residue may be the same structure as the peak recently observed near 10 MeV excitation in a measurement<sup>11</sup> of inelastic scattering of 200-MeV protons from  $^{90}\text{Zr}$ , however, the uncertainty in the residue is large and we cannot confirm the  $(p,p')$  results.

The differential cross sections from the present mea-

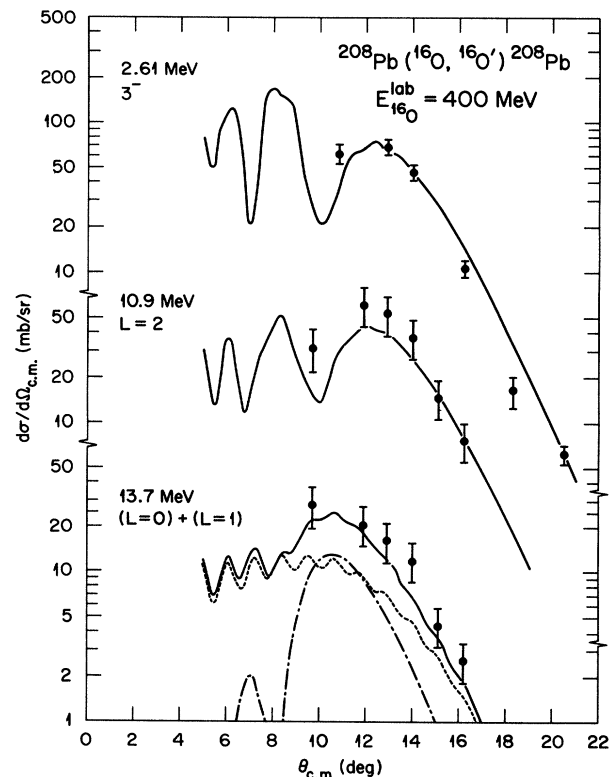


FIG. 7. Measured and calculated angular distributions for indicated states in  $^{208}\text{Pb}$ . The  $3^-$  calculation is normalized to the  $B(E3)$  values measured in Coulomb excitation. The  $L=2$  calculation is normalized to 80% of the  $T=0$ ,  $L=2$  EWSR. The  $L=0$  (short-dash) and  $L=1$  (dash-dot) calculations are normalized to 100% of their respective sum rules.

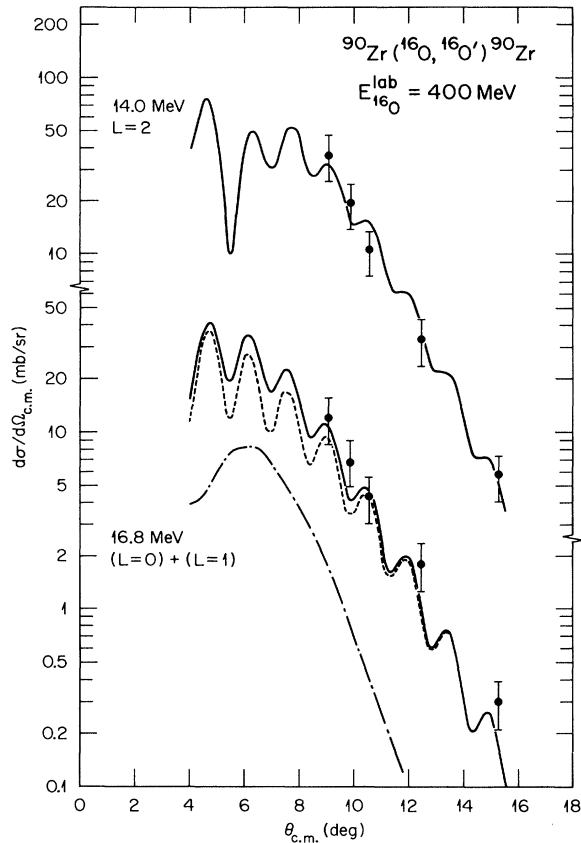


FIG. 8. Measured and calculated angular distributions for indicated giant resonance states in  $^{90}\text{Zr}$ . The  $L=2$  calculation is normalized to 60% of the  $T=0$  EWSR, while the  $T=1, L=1$  (dash-dot) and  $T=0, L=0$  (short-dash) calculations are normalized to 100% of their respective sum rules.

measurements are shown as a function of angle (center of mass) in Figs. 6–8. Figure 6 shows the elastic scattering cross sections relative to the Rutherford cross section. Figure 7 includes the  $^{208}\text{Pb}$  results for the  $3^-$  state at 2.61 MeV, as well as those for the fitted peaks in the giant resonance region at 10.9 and 13.7 MeV excitation. Figure 8 shows the angular distributions for the  $^{90}\text{Zr}$  peaks at 14.0 and 16.8 MeV excitation. The error bars in the differential cross sections indicate the relative uncertainties, which vary between 5% and 15% for the elastics and the 2.61-MeV  $3^-$  state. The relative uncertainties ( $\pm 30\%$ ) on the giant resonance cross sections include a contribution from our estimated uncertainty in the assumed magnitude of the nuclear continuum underlying the giant resonances. There is also an overall normalization uncertainty of  $\sim \pm 10\%$ . For both  $^{90}\text{Zr}$  and  $^{208}\text{Pb}$ , the angular distribution of the continuum underneath the GQR, GMR, and GDR has nearly the same shape as the GR angular distributions.

#### IV. ANALYSIS

##### A. Elastic scattering

The results of optical model fits utilizing the computer code PTOLEMY (Ref. 12) are shown with the elastic data in

TABLE I. Optical model parameters.

Nucleus	$V_r$ (MeV)	$V_i$ (MeV)	$r_0$ (fm)	$a$ (fm)	$r_C$ (fm)
$^{90}\text{Zr}$	40	26	1.15	0.671	1.2
$^{208}\text{Pb}$	60	38	1.17	0.665	1.2

Fig. 6. It was not possible to obtain data inside the grazing angle for  $^{90}\text{Zr}$  because of geometrical limitations. The optical potentials consist of the Coulomb potential between a point charge and a uniformly charged sphere and of nuclear potentials with Woods-Saxon forms for both the real and imaginary parts.

The optical model parameters obtained in the present analysis are included in Table I. These parameters were obtained by setting the real well depth ( $V_r$ ) to a fixed value and allowing the imaginary well depth ( $V_i$ ) to vary along with the radius ( $r_0$ ) and diffuseness ( $a$ ) parameters. The real and imaginary radius and diffuseness parameters were set to be equal. The Coulomb radius parameter was 1.2 fm. Of course these potentials are not unique. Different parameter sets yielding essentially the same reduced chi-squares were obtained by fixing different values of  $V_r$  and  $V_i$ .

##### B. Inelastic scattering

The experimental inelastic scattering angular distributions and the results of DWBA calculations are shown in Figs. 7 and 8 for  $^{208}\text{Pb}$  and  $^{90}\text{Zr}$ , respectively. In this analysis it is assumed that the peak cross sections extracted at 13.7 MeV in  $^{208}\text{Pb}$  and 16.8 MeV in  $^{90}\text{Zr}$  are the sum of the GDR and GMR. The calculations for the 2.61 MeV  $3^-$  state ( $L=3$ ) in  $^{208}\text{Pb}$  and for the GQR ( $L=2$ ) and GDR ( $L=1$ ) resonances in  $^{90}\text{Zr}$  and  $^{208}\text{Pb}$  were made with the computer code PTOLEMY (Ref. 12), in which the standard collective model form factor (i.e., a deformed Woods-Saxon potential) was used for the nuclear part of the effective interaction. For the low-lying  $3^-$  state and the GQR calculations, the Coulomb and nuclear deformation lengths were set equal to each other ( $\beta_n r_0 = \beta_C r_C$ ). It was assumed that the GDR was Coulomb excited only. The GMR ( $L=0$ ) calculations were made with the Oak Ridge version of the computer code DWUCK, in which the form factor for  $L=0$  transitions is similar to that of the standard collective model, but is supplemented by a volume conserving term suggested by Satchler.<sup>13</sup> The  $L=0$  and  $L=1$  calculations are denoted by short-dash and dash-dot-dash curves, respectively, in Figs. 7 and 8.

The DWBA calculations for the  $3^-$  state in  $^{208}\text{Pb}$  were made with a deformation of  $\beta=0.110$ , which corresponds to  $B(E3)=0.600 e^2 b^3$ . This value is in good agreement with experimental  $B(E3)$  values.<sup>14</sup> As shown in Fig. 7, there is reasonable agreement between the experimental and calculated angular distributions for the  $3^-$  state. Several additional calculations for the  $3^-$  state were made with different optical potentials, which were obtained from the elastic scattering cross sections by using different values of  $V_r$  and  $V_i$  and allowing  $r$  and  $a$  to vary. The various potentials typically produced inelastic cross sec-

tions at the grazing angle within 20% of that shown in Fig. 7. However, at the larger angles the cross sections differed with that in Fig. 7 by up to a factor of 2. The giant resonance calculations shown in Figs. 7 and 8 are normalized to energy-weighted sum rule (EWSR) strengths, which have been determined in previous measurements.<sup>1</sup> For the GQR we used 80% and 60% of the EWSR for  $^{208}\text{Pb}$  and  $^{90}\text{Zr}$ , respectively. For the remaining resonances, we used 100% of the appropriate EWSR.

## V. DISCUSSION AND CONCLUSIONS

The agreement between the calculation and the data for the  $3^-$ , 2.61 MeV state in  $^{208}\text{Pb}$ , although somewhat parameter dependent, gives us confidence that giant resonance sum rule strength can be properly deduced from heavy-ion inelastic scattering. For both  $^{208}\text{Pb}$  and  $^{90}\text{Zr}$ , the agreement between the measured and calculated cross sections for the GQR peak and GDR + GMR peak is excellent using  $B(EL)$  values obtained from previous hadronic inelastic scattering. We have assumed that the 13.7 MeV resonance peak in  $^{208}\text{Pb}$  and the 16.8 MeV peak in  $^{90}\text{Zr}$  are composed of excitation of both the  $T=1$  GDR and  $T=0$  GMR; the GDR would be excited through Coulomb excitation since  $^{16}\text{O}$  is a  $T=0$  projectile. For  $^{208}\text{Pb}$  it is clear that the  $L=0$  calculation with 100% EWSR cannot account for the measured cross sections at all angles. However, inclusion of 100% of the  $L=1$  calculation provides excellent agreement with the data. In the case of  $^{90}\text{Zr}$ , however, the data can be explained equally well by either the  $L=0$  calculation alone or by the sum of  $L=0$  and  $L=1$ .

Recently, 10% of the  $T=0$ ,  $L=4$  EWSR has been found<sup>15</sup> at an excitation energy of 12.0 MeV in  $^{208}\text{Pb}$ . We calculate that a cross section of  $\sim 10$  mb/sr would be expected for excitation of this resonance in our 400 MeV ( $^{16}\text{O}, ^{16}\text{O}'$ ) data. This is only  $\sim \frac{1}{6}$  of the observed cross section of the 10.9-MeV GQR resonance. Because the angular distributions for  $L=2$  and  $L=4$  excitations in heavy-ion inelastic scattering at 25 MeV/nucleon are essentially identical, the  $L=4$  resonance in the ( $^{16}\text{O}, ^{16}\text{O}'$ ) spectra is completely obscured by the much stronger GQR. The nearly identical shapes of the low  $L$ -transfer angular distributions (see Fig. 7, for example) provide what is perhaps the most serious drawback to heavy-ion inelastic excitation of giant resonances. Identification of resonance multipolarity, via angular distributions, is not possible, at least for heavy ions up to 25–30 MeV/nucleon.

It is largely because the shapes of the angular distribution are not sensitive to the angular momentum transfer that we have not been able to determine whether the 17.6 MeV peak in  $^{208}\text{Pb}$  and the 23 MeV peak in  $^{90}\text{Zr}$  are giant resonances. These peaks appear in the spectra at all measured angles, and calculations indicate that it is unlikely that the peaks arise from mutual excitation of the projectile and target nuclei. In addition, the peak at 17.6 MeV in  $^{208}\text{Pb}$  may possibly be due to the decay of pickup channels.

However, for  $^{208}\text{Pb}$ , the energy (17.6 MeV) and width (4.0 MeV) of the peak in our spectra agree with an ( $\alpha, \alpha'$ )

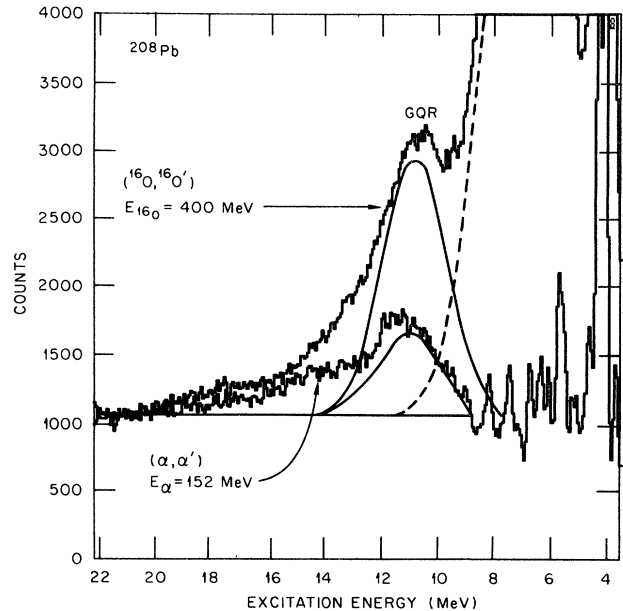


FIG. 9. Comparison of  $^{208}\text{Pb}$  giant resonance spectra as obtained from the ( $^{16}\text{O}, ^{16}\text{O}'$ ) reaction at 400 MeV and the ( $\alpha, \alpha'$ ) reaction at 152 MeV. The spectra are normalized at 22-MeV excitation.

study<sup>16</sup> at  $E_\alpha = 172$  MeV, in which strength at 17.6 MeV is interpreted as the  $3\hbar\omega$  isoscalar giant octupole resonance (GOR) depleting about 60% of the EWSR. If we interpret the 17.6 MeV peak in our  $^{208}\text{Pb}$  data as arising from excitation of the GOR, then at  $12^\circ$  the peak cross section accounts for  $\sim 40\%$  of the EWSR, a value not inconsistent with the ( $\alpha, \alpha'$ ) results. However, medium energy proton inelastic scattering measurements<sup>17,18</sup> in  $^{208}\text{Pb}$  find the GOR at  $\sim 19$ – $20$  MeV. Indeed, in the 200 MeV ( $p, p'$ ) measurements of Ref. 18 no peak is found at 17.6 MeV, in disagreement with both the ( $\alpha, \alpha'$ ) measurements of Ref. 16 and the present heavy-ion measurement.

The most important feature of the heavy-ion inelastic excitation of giant resonances is the large resonance cross section and large peak to continuum ratio observed. As shown in Fig. 7 for  $^{208}\text{Pb}$ , the GQR cross section reaches  $\sim 60$  mb/sr at the grazing angle,  $\sim 6$ – $7$  times larger than realized in 200 MeV ( $p, p'$ ) scattering and nearly twice as large as that obtained in 152 MeV ( $\alpha, \alpha'$ ) measurements.<sup>19</sup> A comparison between the giant resonance spectra in  $^{208}\text{Pb}$  from the present heavy-ion measurements and the 152 MeV ( $\alpha, \alpha'$ ) measurements<sup>19</sup> on  $^{208}\text{Pb}$  is shown in Fig. 9. The two spectra are normalized at 22 MeV of excitation energy. The solid line drawn under both spectra indicates only an approximate “background” level for comparing the two spectra. The solid curves in each spectrum are the shape of the GQR peak. As was discussed earlier, the heavy ion spectrum contains a very large peak from excitation of states in the  $^{16}\text{O}$  projectile. This effect is, of course, not present in the alpha particle scattering, so that much more structure is seen below the giant resonance peak. The most obvious difference in the two spectra is the very much larger peak to continuum ratio in the case of the heavy-ion scattering. This ratio is over twice that

observed with alpha particles. Although the heavy-ion cross sections are somewhat larger than for alpha-particle scattering, much of the improved peak to continuum ratio comes from a reduced continuum cross section.

Based on our present data it seems fair to say that heavy-ion excitation of giant resonances provides mixed results. On the positive side, the resonances are excited with large cross sections, and more importantly, the peak to continuum ratio is extremely large. Furthermore, rather standard collective model calculations properly account for the observed cross section. On the negative side, heavy-ion angular distributions offer little hope for use in multipolarity identification. In addition, strong excitation of states in the projectile tend to confuse the giant resonance spectra, as does the large cross section for pick-up reactions.

The positive aspects to heavy-ion giant resonance excitation, i.e., the large cross sections and outstanding peak to continuum ratio, offer significant advantages over light ions for measurements of the decay of the giant resonances.

#### ACKNOWLEDGMENTS

One of us (T.P.S.) would like to thank G. R. Satchler for helpful discussions and M. J. Rhoades-Brown for modifying PTOLEMY so that it could properly calculate the  $T=1$ ,  $L=1$  cross sections in  $^{208}\text{Pb}$  at 400 MeV. Oak Ridge National Laboratory is operated by Union Carbide Corporation under Contract W-7405-eng-26 with the U.S. Department of Energy.

---

\*Present address: Computer Science Department, University of Illinois, Urbana, IL 61801. (Oak Ridge Summer Research Participant.)

<sup>1</sup>F. E. Bertrand, in Proceedings of the International Conference on Nuclear Physics, Berkeley, 1980, Nucl. Phys. **A354**, 129c (1981).

<sup>2</sup>*Giant Multipole Resonances*, edited by F. E. Bertrand (Harwood, New York, 1980).

<sup>3</sup>J. Speth and A. van der Woude, Rep. Prog. Phys. **44**, 46 (1981).

<sup>4</sup>F. E. Bertrand, in *Proceedings of the International School of Physics "Enrico Fermi" Course LXXVII on Nuclear Structure and Heavy-Ion Collisions, Varenna, Italy, 1979*, edited by R. A. Broglia, R. A. Ricci, and C. H. Dasso (North-Holland, Amsterdam, 1981), p. 620.

<sup>5</sup>A. M. Sandorfi, Proceedings of the Symposium on Heavy-Ion Physics from 10 to 200 MeV/amu, 1979, Brookhaven National Laboratory, Report No. BNL-51115, 1979, Vol. 1, p. 405 (unpublished).

<sup>6</sup>R. Kamermans, J. van Driel, H. P. Morsch, J. Wilczynski, and A. van der Woude, Phys. Lett. **82B**, 221 (1979); M. Buenerd, D. Lebrun, J. Chauvin, Y. Gaillard, J. M. Loiseaux, P. Martin, G. Perrin, and P. de Saintignon, Phys. Rev. Lett. **40**, 1482 (1978); H. J. Gils, H. Rebel, J. Buschmann, and H. Klewe-Nebenius, Phys. Lett. **68B**, 427 (1977).

<sup>7</sup>P. Doll, D. L. Hendrie, J. Mahoney, A. Menchaca-Rocha, D. K. Scott, T. J. M. Symons, K. Van Bibber, Y. P. Viyogi, and H. Wieman, Phys. Rev. Lett. **42**, 366 (1979).

<sup>8</sup>U. Garg, P. Bogucki, J. D. Bronson, Y.-W. Lui, K. Nagatani, E. Takada, N. Takahashi, T. Tamaya, and D. H. Youngblood, Phys. Lett. **93B**, 39 (1980).

<sup>9</sup>W. T. Milner, J. A. Biggerstaff, D. C. Hensley, and R. O. Sayer, IEEE Trans. Nucl. Sci. **NS-26**, 4399 (1979); W. H. Atkins, *ibid.* (to be published).

<sup>10</sup>A. Kiss, C. Mayer-Boricke, M. Rogge, P. Turke, and S. Wiktar, Phys. Rev. Lett. **37**, 1188 (1976), and references therein.

<sup>11</sup>J. R. Tinsley (private communication).

<sup>12</sup>M. Rhoades-Brown, M. H. Macfarlane, and Steven C. Pieper, Phys. Rev. C **21**, 2417 (1980); **21**, 2436 (1980); M. H. Macfarlane and S. C. Pieper, Argonne National Laboratory Report No. ANL-76-11, Rev. 1, 1978 (unpublished).

<sup>13</sup>G. R. Satchler, Part. Nucl. **5**, 105 (1973).

<sup>14</sup>E. E. Gross, J. R. Beene, K. A. Erb, M. P. Fewell, D. Shapira, M. J. Rhoades-Brown, G. R. Satchler, and C. E. Thorn, Nucl. Phys. **A401**, 362 (1983), and references therein.

<sup>15</sup>J. R. Tinsley, D. K. McDaniels, J. Lisantti, L. W. Swenson, R. Liljestrang, D. M. Drake, F. E. Bertrand, E. E. Gross, D. J. Horen, and T. P. Sjoreen, Phys. Rev. C **28**, 1417 (1983).

<sup>16</sup>H. P. Morsch, M. Rogge, P. Turek, and C. Mayer-Boricke, Phys. Rev. Lett. **45**, 337 (1980).

<sup>17</sup>T. A. Carey, W. D. Cornelius, N. J. DiGiacomo, J. M. Moss, G. S. Adams, J. B. McClelland, G. Pauletta, C. Whitten, M. Gazzaly, N. Hintz, and C. Glashauser, Phys. Rev. Lett. **45**, 239 (1980).

<sup>18</sup>D. K. McDaniels, J. R. Tinsley, J. Lisantti, D. M. Drake, I. Bergqvist, L. W. Swenson, F. E. Bertrand, E. E. Gross, D. J. Horen, T. P. Sjoreen, R. Liljestrang, and H. Wilson, Phys. Rev. C (to be published).

<sup>19</sup>F. E. Bertrand, G. R. Satchler, D. J. Horen, J. R. Wu, A. D. Bacher, G. T. Emery, W. P. Jones, D. W. Miller, and A. van der Woude, Phys. Rev. C **22**, 1832 (1980).